PHYSICAL REVIEW E, VOLUME 63, 035302(R)

Shock wave criterion for propagating solitary states in driven surface waves

O. Lioubashevski and J. Fineberg
The Racah Institute of Physics, The Hebrew University of Jerusalem, Jerusalem 91904, Israel
(Received 12 November 2000; published 13 February 2001)

Highly localized solitary states are observed to propagate along the surface of a thin two-dimensional fluid layer. The states are driven by means of a spatially uniform, temporally periodic, vertical acceleration (Faraday experiment) in a highly dissipative fluid. These states are shown to be formed by coupled fronts that propagate, periodically, as shock waves. A criterion for their formation based on shock initiation is presented. Both the characteristic form and interaction dynamics of the solitary states can be understood in this picture.

DOI: 10.1103/PhysRevE.63.035302 PACS number(s): 47.20.Gv, 47.20.Ky, 47.35.+i, 47.54.+r

The concept of solitary states can be found in many branches of physics. Solitonlike localized structures are ubiquitous in one-dimensional (1D) integrable systems but are rarely observed in dissipative 2D or 3D systems; hence, little is known about their formation and behavior. Recent studies of extensions to the conservative Kuramoto-Sivashinsky and KdV equations [1] show that dissipation strongly influences solitons. Although solitonlike solutions were seen to persist, a small amount of dissipation was enough to cause the collapse of a family of solitons having a continuum of propagation velocities to a single selected state. Solitonlike localized states [2] and localized oscillon solutions [3] have been seen in the complex Ginzburg-Landau equation, a 2D system with dissipation and dispersion. Physically such solutions exist due to balances between either dispersion and nonlinearity or nonlinear amplification and dissipation.

Experimentally, propagating temporally intermittent localized states in 2D dissipative systems have been observed in convecting binary mixtures [4] and catalytic oxidation of CO on a 2D substrate [5]. Stable propagating solitary states (PSS) occur both on the surface of a spatially uniform, periodically accelerated thin fluid layer of viscous fluid [6] and in colloidal suspensions [7], where parametrically excited oscillons [8] undergo a transition to PSS. In contrast to classical solitons that tend to be destroyed upon the introduction of dissipation, PSS occur solely in *highly* dissipative systems. Below we will elucidate the governing mechanism for the transition from standing waves to PSS and show that the criterion for PSS creation coincides with shock wave formation. We will then show that this scenario provides an explanation for both the intriguing form of PSS and their interesting behavior upon collision.

Our experimental system, described at length in Ref. [6], is generally used to study the Faraday instability. We drive the system by spatially uniform acceleration of a fluid layer in the vertical (parallel to gravity, g) direction with a displacement $z(t)=a/\omega^2 \sin(\omega t)$, where a and ω are the applied acceleration and angular frequency. The system is further characterized by h, ν, ρ, and σ defined, respectively, as the fluid depth, kinematic viscosity, fluid density, and surface tension. We performed our experiments in a 14.4 cm diameter circular cell mounted on a mechanical shaker providing vertical acceleration from $0-30g$ over a frequency range of 14–80 Hz (providing cell diameter to wavelength ratios of 7–30). Newtonian fluids (properties are described in Ref. [6], and they can be obtained from the Kurt J. Lesker Company) TKO-FF, TKO-300, and TKO-77 were used with $0.1<h<0.6$ cm σ and ν were varied between 29.6–31.0 dyn/cm and 0.25–6.7 St, respectively. We determined the instability onset by shadowgraph visualization. Direct visualization of the propagating states was performed by scattered stroboscopic light viewed either from the side or above at video frame-rates (using a JAI MV-30) of 60–360 Hz.

The driving frequency $f=\omega/(2\pi)$ and dimensionless acceleration amplitude, $\Gamma=a/g$, can be viewed as the system's control parameters. Experiments were performed by fixing f and adiabatically increasing a. At a critical value, Γ_c, the initially uniform fluid state loses its stability to a stable, (worm-like) elongated confined state. This confined state (lower right, Fig. 1) is composed of short stripes of stationary standing waves oscillating at $f/2$ with a slow spatial modulation of the wave amplitude in the direction normal to their crests.

Upon further increase of Γ, the confined state loses its stability in one of two scenarios depending on the value of the dimensionless parameter, δ/h, where $\delta=(\nu/\omega)^{1/2}$ is the viscous boundary layer depth. For $\delta/h<0.37$, the confined

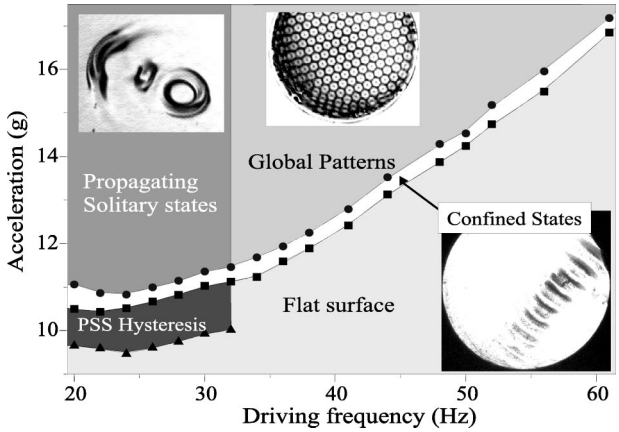

FIG. 1. A typical phase space of parametrically driven surface waves in highly dissipative fluids. Transitions upon increasing Γ and hysteretic regions of PSS are indicated. Transitions to confined patterns (squares) and PSS/patterns (circles) with PSS hysteresis (triangles) are shown ($\nu=3.39St$, $h=0.38$ cm). Insets: Views from above of PSS, global and confined patterns.

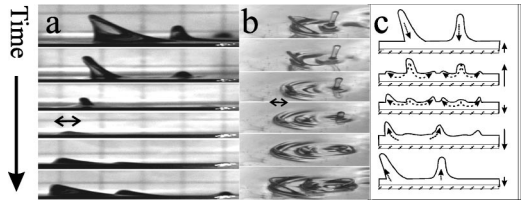

FIG. 2. PSS, propagating from right to left; (a) side and (b) angled views. Here $f=30$ Hz, $\nu=3.39$ cm^2/s (St) and $h=0.38$ cm with 4.2 msec between frames. The vertical dimension, indicated by the 1 cm grid, is scaled to half of the horizontal one. Double arrows indicate R_{jump} (see text). (c) A schematic view of the fluid flow within a PSS.

state expands and results in global subharmonic pattern similar to those observed in previous work [9]. For $\delta/h>0.37$, the system bifurcates to PSS for Γ typically a few percent above Γ_c. PSS have a large initial amplitude and propagate with a single mean velocity for given values of h, ν and ω. When PSS are excited, no extended wave patterns are observed. The transition to PSS is hysteretic (Fig. 1), with PSS persisting 10–15 % below Γ_c.

The typical structure of PSS as a function of time (Fig. 2) is independent of both the fluid parameters and ω. Unlike the confined states, PSS reproduce their form at the driving frequency, f. This state consists of a curved leading front followed by a ''finger'' of fluid and ending with a low ridge of fluid whose curvature is opposite that of the leading front. The fluid directly preceding the state is undisturbed. Upon formation, a PSS propagates along a straight line until destroyed by collisions with either another PSS or the lateral boundaries. Reflections of PSS from the lateral boundaries may also occur.

The position of the leading edge of a PSS as function of time is presented in Fig. 3(a). In every driving period the PSS lateral motion occurs in two phases: a rapid jump of size R_{jump} [indicated by the arrows in Figs. 2(a) and 2(b)] followed by slow wavelike propagation. R_{jump} scales with ν/h (see inset). $R_{jump}/(\nu/h)$, which has dimensions of time, has no additional ν or ω dependence. The jump duration (5–10 msec) is similar to the spreading time of viscous drops impinging on a rigid surface [10] and 5–10 times less than $R_{jump}/(\nu/h)$ (55 msec).

In Figs. 3(b) and 3(c) we compare the vertical (relative to the cell's bottom plate) and lateral motions of the leading edge of a typical PSS. The PSS peaks when the plate is approximately at its minimum, with the PSS lagging a_{min} by 20°–40°. The PSS maximum amplitude, A_{max}, is equal to about twice the plate stroke, $A_{max}\sim 2a/\omega^2$.

In Fig. 3(c) we show the time dependence of the instantaneous lateral velocity of a typical PSS. During its slow propagation phase, the wave progresses at velocities of about half the phase velocity (ω/k) of surface waves. In the short phase of rapid propagation, PSS propagate nearly an order of magnitude faster, with maximal lateral velocities occurring near their minimum amplitude. The sharp increase in PSS velocity occurs just after the upward maximal velocity of the plate, as the PSS's peak seems to ''impact'' the plate.

These observations suggest a mechanism for PSS formation from standing waves. Let us first consider the motion of a standing wave in a low viscosity fluid ($\Gamma_c\ll 1$) whose amplitude is much lower than h. In the rest frame of an upwardly accelerating plate, an initial upward protrusion of the fluid surface is accelerated downward towards the plate. The momentum within this fluid drives it below the fluid surface, laterally displacing the fluid beneath it. As long as the amplitude of the wave is much smaller than the fluid depth, the effect of the bottom plate is negligible and the wave that forms is, to a good approximation, sinusoidal.

The wave motion changes drastically when $\Gamma\gg 1$ and the wave amplitude exceeds the fluid depth. In both oscillon formation in two frequency driving [11] and the formation of pendant drops [12], a shape-changing transition to high-amplitude, fingerlike waves occurs beyond a critical wave amplitude. A similar effect occurs in this system. Beyond a critical amplitude, the low amplitude confined state loses stability to waves whose amplitude is much larger than h. When the wave amplitude is sufficiently large, PSS formation occurs. This is qualitatively illustrated in Fig. 2(c). Let us consider an initial large-amplitude wave [Fig. 2(c),top], which occurs when the bottom plate is near its minimum height. As the plate accelerates upward, the fluid within the wave is rapidly accelerated toward the rigid bottom. In a shallow fluid layer, the high momentum carried by the wave is not dissipated before the fluid reaches the bottom plate. Upon interaction with the plate, the displaced fluid is diverted to a

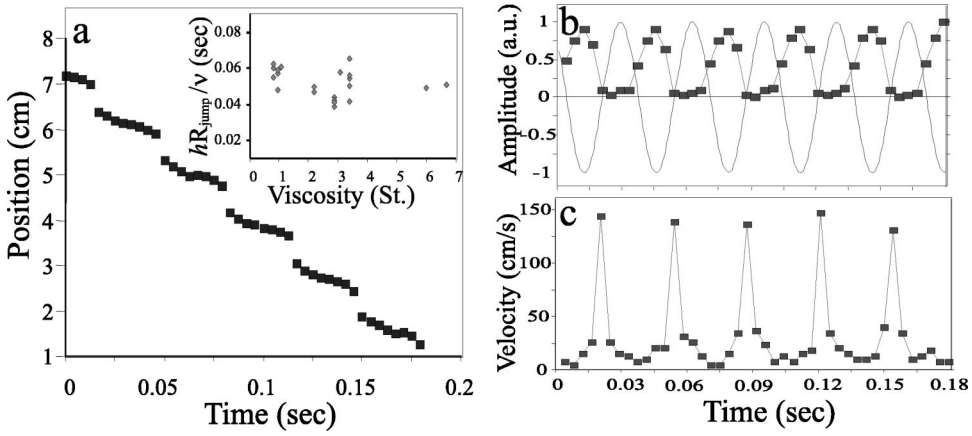

FIG. 3. (a) PSS leading front position versus time. Inset: $R_{jump}/(\nu/h)$ vs ν. (b) Temporal behavior of the normalized amplitude, $A(t)/A_{max}$, of the leading edge (solid squares) vs plate position (solid line). (c) The instantaneous lateral velocity of a PSS with time. $f=30$ Hz, $\nu=3.39$ St, $h=0.38$ cm. Inset: $f=20$–40 Hz, $h=0.15$–0.38 cm.

rapid, laterally moving front [Fig. 2(c), 2nd and 3rd frame] not evident in a pure standing wave state. A similar interaction causes rapid *crater-like* cylindrical fronts that are formed when a fluid drop impacts a rigid surface [10]. In both PSS formation and fluid-drop impact, this phase of rapid lateral motion is quickly damped (within ~ 10 ms) due to both shear with the lower boundary and surface tension which opposes the large curvature at the tip of the front. The front now only slowly propagates laterally. It is, however, vertically amplified as the plate accelerates downward, since, for $a > g$, a Rayleigh-Taylor type mechanism [13,14], occurs [Fig. 2(c), 4th and 5th frame]. Continuing lateral propagation of the PSS will occur when the amplitude of the laterally moving front becomes large enough to generate a new front at the next forcing period. Thus, a high-amplitude standing wave accelerated into the fluid results in shock-like moving front upon impact with the plate.

The structure of a PSS is now apparent. Upon impact, a curved high-amplitude front will generate two new fronts: a forward-propagating one of increasing radius and a backward-propagating converging front. The first front becomes the leading edge of the PSS, while the second front is focused into the fingerlike trailing wave apparent in Fig. 2. On successive impacts each high-amplitude leading front generates both a new leading edge and a new trailing ''finger.'' The impact of the finger with the bottom plate creates the nearly circular ''craterlike'' structure (see, e.g., the view of a PSS presented in Fig. 1) at the trailing edge of the PSS.

In the above picture, a necessary condition for the formation of PSS is the formation of rapidly propagating sharp fronts upon impact with the bottom plate. The fact that the lateral velocity (130 cm/s in Fig. 3) of the leading edge significantly exceeds the surface wave group velocity [15,19] ($v_g \sim 70$ cm/s for the parameters of Fig. 3) suggests that these fronts are shock waves. This suggestion is strengthened by studies [16] of fluid-drop impact showing that low-velocity impact results in fluid spreading and surface wave excitation, whereas at high impact velocities a threshold exists for leading edge jumps that correspond, theoretically, to shock waves.

Is shock wave formation a *sufficient* condition for PSS creation? Our video rate is too slow to enable precise measurements of V_{PSS}, the instantaneous propagation velocity of PSS. V_{plate}, the maximal plate velocity, however, provides a good estimate of V_{PSS} and can be measured to high precision. Using the numerical code developed by Kumar and Tuckerman [17], v_g can be calculated for any desired values of the system parameters ω, ν, h, and ρ. If shock wave formation is indeed a sufficient condition for PSS, we would expect the transition to PSS to occur when $V_{PSS} \sim v_g$, or equivalently, for a critical value of V_{plate}/v_g. In Fig. 4 we plot the value of this ratio at the transitions from patterns to PSS for experiments performed over a wide range of ω, ν, and h. As the figure shows, the criterion $V_{plate}/v_g = 1$ is in excellent agreement with the measured transitions.

Previous work [6] has shown that the transition from patterns to PSS occurs at a critical value of $(\delta/h) \sim 0.37$. For comparison, the value of δ/h at the transition is also plotted in Fig. 4. As the figure shows, this criterion is also consistent

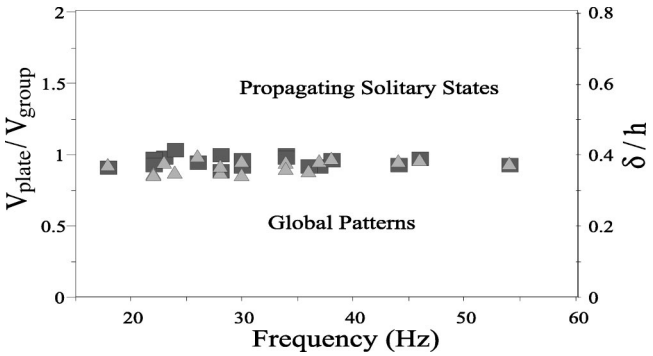

FIG. 4. Solid squares, the ratio of the maximal plate velocity, V_{plate}, to the fluid group velocity, v_g; and triangles (δ/h) at the transition to PSS as functions of a_c. $0.25 < \nu < 6.7$ St, $0.1 < h < 0.6$ cm.

with the transition. We will now show that the two criteria are roughly equivalent in the range of parameters that is experimentally accessible. In this parameter range, a good approximation [13] for Γ_c is $\Gamma_c = a_c/g \sim 15\pi\nu^2/(h^3 g)$. Thus [18], $V_{plate} = a_c/\omega \sim 15\pi\nu^2/(h^3\omega)$. As shock formation occurs very near the maximal value of a, the instantaneous value of the effective gravity at the moment of shock formation is, to a good approximation, a_c. At this moment, the instantaneous value of v_g, estimated using the shallow fluid approximation, is $v_g \sim (a_c h)^{1/2}$ (accurate to within 20%). With these approximations, $V_{plate}/v_g = (15\pi)^{1/2}(\delta/h)^2$ and the condition $V_{plate} = v_g$ for the transition to PSS yields a value of $(\delta/h)_c$ 0.4. This estimate agrees well with the experimental value of $(\delta/h)_c = 0.37$. Although the two criteria are roughly equivalent in this region of phase space, regions where it should be possible to differentiate between them are experimentally inaccessible with our present equipment. We feel, however, that the shock formation criterion provides an accurate intuitive picture for the transition that complies well with the PSS structure described earlier.

Unlike classic solitons, whose interaction results in a simple phase change, interactions of PSS states reveal a much richer behavior. Upon colliding, two counterpropagating PSS states can either interpenetrate, mutually annihilate or, for a nonzero impact parameter, merge into a metastable bound state that decays via emission of two new PSS. Typical examples of interpenetration and mutual annihilation are presented in Fig. 5. We will now use our picture of PSS evolution to understand PSS behavior upon collision. As (Fig. 3) PSS are temporally locked to the driving, all states have the same *temporal* phase. Their relative *spatial* location, however, is arbitrary. Let us consider the schematic representation of PSS phases described in Fig. 2(c). If two counterpropagating PSS meet while in their rapid propagation phase [Fig. 2(c),center], the interference inherent in the two opposing rapid lateral flows may tend to effectively damp the fluid motion. Thus, we would expect that if two PSS meet during the ''shock'' phase of their motion, mutual annihilation will occur, as shown in Fig. 5(a). If, on the other hand, two PSS collide when they are in their slowly propagating phase [i.e., when the fluid motion is primarily vertical, as in the top and bottom frames of Fig. 2(c)], the fluid mo-

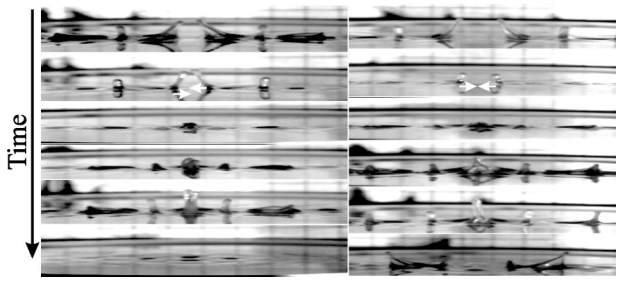

FIG. 5. Head-on collisions of two counterpropagating solitary states showing (right) interpenetration and (left) mutual annihilation. Arrows indicate the points to which the next PSS jump would occur. When collisions occur *within* a jump, annihilation takes place. Full periods of PSS motion prior to the final state are displayed, with 8.4 msec between all subframes except the last which is separated by a 100 msec interval.

tions of both interacting PSS will be complementary. In this case, little interference will occur, and we should expect the PSS states to pass through each other, as in Fig. 5(b). This picture is consistent with all observed collisions (typified by Fig. 5) and is supported by measurements of the maximal amplitude of the merged fronts at the *moment* of interaction (see subframe 4 in Fig. 5), which are at least 60% larger in PSS interpenetration than when annihilation occurs. Thus, as in Ref. [2], the outcome of a collision between two PSS is determined by their relative phase at the moment of interaction.

In conclusion, we have shown that the unique form of propagating solitary states results from interacting fronts. These fronts are created by shock waves, formed as a result of the interaction of high-amplitude standing waves with the lower boundary of the system. We have shown that shock wave formation is a sufficient condition for PSS formation. This picture both explains both the structure of single PSS states and the types of interaction that two colliding PSS can undergo. We still lack a quantitative theoretical description of these states. The absence of both confined and PSS states in recent simulations of the 2D Navier-Stokes equations [20] has shown that 3D effects must be taken into account. It remains to be seen whether these states can be successfully modeled.

J.F. and O.L. wish to acknowledge the support of the Israel Academy of Science Grant No. 203/99.

[1] See, e.g., C. I. Christov and M. G. Velarde, Physica A **323**, 47 (1995).

[2] R. J. Deissler and H. R. Brand, Phys. Rev. Lett. **74**, 4847 (1995); Phys. Rev. A **44**, 3411 (1991).

[3] H. Sakaguchi and H. R. Brand, Europhys. Lett. **38**, 341 (1997); Physica D **117**, 95 (1998); C. Crawford and H. Riecke, *ibid.* **129**, 83 (1999); L. S. Tsimring and I. S. Aranson, Phys. Rev. Lett. **79**, 213 (1997).

[4] V. Steinberg, J. Fineberg, E. Moses, and I. Rehberg, Physica D **37**, 359 (1989); K. Lerman, E. Bodenschatz, D. S. Cannell, and G. Ahlers, Phys. Rev. Lett. **70**, 3572 (1993).

[5] H. H. Rotermund, S. Jakubith, A. von Oertzen, and G. Ertl, Phys. Rev. Lett. **66**, 3083 (1991).

[6] O. Lioubashevski, H. Arbell, and J. Fineberg, Phys. Rev. Lett. **76**, 3959 (1996).

[7] O. Lioubashevski, Y. Hamiel, A. Agnon, Z. Reches, and J. Fineberg, Phys. Rev. Lett. **83**, 3190 (1999).

[8] P. Umbanhowar, F. Melo, and H. L. Swinney, Nature (London) **382**, 793 (1996).

[9] W. S. Edwards and S. Fauve, J. Fluid Mech. **278**, 123 (1994); J. Bechhofer, V. Ego, S. Mannevile, and B. Johnson, *ibid.* **288**, 325 (1995).

[10] T. Mao, D. Kuhn, and H. Tran, AIChE J. **43**, 2169 (1997).

[11] H. Arbell and J. Fineberg, Phys. Rev. Lett. **85**, 756 (2000).

[12] E. D. Wilkes and O. A. Basaran, J. Fluid Mech. **393**, 333 (1999); A. D. Myshkis, V. G. Babskii, N. D. Kopachevskii, L. A. Slobozhanin, and A. D. Tyuptsov, *Low-Gravity Fluid Mechanics* (Springer-Verlag, Berlin, 1987).

[13] O. Lioubashevski, L. Tuckerman, and J. Fineberg, Phys. Rev. E **55**, 3832 (1997).

[14] S. Kumar, Phys. Rev. E **62**, 1416 (2000).

[15] v_g was obtained by numerical derivation of $\omega(k)$, where ω is the driving frequency and k the critical wave number for parametric excitation. This value of v_g was within 10% of that given by the shallow fluid approximation [19],$(a_c h)^{1/2}$.

[16] A. L. Yarin and D. A. Weiss, J. Fluid Mech. **283**, 141 (1995); B. L. Scheller and D. W. Bousfield, AIChE J. **41**, 1357 (1995).

[17] K. Kumar and L. S. Tuckerman, J. Fluid Mech. **279**, 49 (1994).

[18] In [13] a_c in the highly dissipative regime was fit by: $a_c(2/\pi - g/a_c)/\omega^2 h = 0.1 + 30(\delta/h)^4$. For $\Gamma_c \gg 1$, Γ_c $15\pi(\nu^2/h^3 g)$.

[19] For our experimental conditions, $kh \sim 1$. The gravity wave approximation here is justified, since surface tension [13] in this parameter range plays a negligible role.

[20] Y. Murakami, Phys. Fluids (to be published).